Gain characteristics of inner-shell photoionization-pumped $L_{23}M_1$ transition in Ca

D. Kim,[1] S. H. Son,[1] J. H. Kim,[1] C. Tóth,[2] and C. P. J. Barty[2]

[1]*Pohang University of Science and Technology, Pohang, 790-784, Republic of Korea*
[2]*University of California, San Diego, La Jolla, California 92093-0339*

A new physical scheme for femtosecond x-ray lasers, where the upper lasing level (L_{23} innershell vacancy level) is pumped by x-ray photons and the lower lasing level (M_1 innershell vacancy level) is depopulated via a Coster–Kronig radiationless transition, is analyzed for Ca. The transition wavelength is 4.1 nm, which is inside the water window (the wavelength range between the K absorption edges of oxygen and carbon). The peak spectral brightness of the x-ray laser output at 4.1 nm is predicted to be as large as 5×10^{25} photons/s/(mm^2 mrad^2 0.1% bandwidth), which is 4 to 5 orders of magnitude brighter than a typical undulator radiation in the similar spectral region. In addition to the high flux, the expected duration of x-ray lasing of ~ 3 fs will be useful for the study of fast dynamics in physical and biological sciences.

PACS number(s): 42.55.Vc, 32.80.Hd, 34.80.Gs, 52.25.Os

New regimes of laser matter interaction have opened due to recent advances in the 10 fs range, high-peak-power laser development [1–4]. These lasers are ideal for the generation of femtosecond high-order harmonic radiation in the soft x-ray range [5–9], and for pumping x-ray lasers based on innershell atomic transitions [10–16]. While the past 15 years have seen significant progress in the x-ray laser research and development, most x-ray lasers operate at low-repetition rates with pulses in picoseconds or longer. High-repetition-rate, femtosecond x-ray lasers would be useful for dynamical studies of ultrafast phenomena in nature [17].

Duguay and Rentzepis [18] first proposed inner-shell x-ray laser schemes in 1967. In their scheme the lower level of the lasing transition was the ground level of the first ion and could not decay. The idea of using an atomic system in which the lower level decays was suggested by Stankevich [19], elaborated by Arecchi [20] and Elton [21], and calculated in detail by Axelrod for K-shell transitions [22]. The technical barrier for the successful realization of these schemes has been the development of a sufficiently fast and energetic x-ray pump source whose time scale is on the order of the lifetime of the keV lasing transitions, i.e., in the 10 fs range [10,11,15,22]. Such pumping sources are now becoming available due to the advent of femtosecond ultrahigh peak-power lasers. Such systems with peak powers of tens to hundreds of terawatt (TW) have been demonstrated [1–4] and plans exist for extending peak powers to 1 petawatt at a 20-fs pulse duration. Even with these new lasers, intrinsic problems with the K-shell transition x-ray laser scheme still exist. In particular, electrons produced during photoionization and subsequent Auger decays are energetic enough to collisionally ionize neutral atoms, producing the lower level of the lasing transition and destroying the inversion. If it were possible to create an inner-shell population inversion via atomic processes involving only electrons, the inversion in any photoionization pumped x-ray laser schemes based on the same transitions would be (1) much less sensitive to secondary electron-collisional filling of the lower level, and (2) maintained longer, compared to equivalent photo-inner-shell ionization pumping schemes for the KL transition.

Recently Kim *et al.* have investigated pairs of inner-shell-vacancy levels (IVL's) for x-ray lasers in which the lower level rapidly decays through Coster–Kronig and super-Coster–Kronig processes [10]. These processes are extremely fast so that the lifetime of the lower level is much shorter than that of the upper level. Surveys of possible transition pairs noted that the $L_{23}M_1$ transition in the elements of $Z=20$ to 30 should be the best candidate for large population inversion. Numerical simulations have shown that a population inversion between the L_{23} and M_1 IVL's can be created even by only electron collisional ionization processes. Due to the larger electron collisional ionization cross sections for all outershells, it is not possible to create an instantaneous inversion between the IVL's by only direct electron collisional ionization. Inversion can be achieved, however, on a transient basis via the fast decay of the lower level. In the case of photoionization pumping, the situation is reversed; the ionization cross sections are larger for innershells than for outershells if the energy of a pumping photon is larger than the ionization threshold of the particular innershell. Hence the degree of initial inversion between the L_{23} and M_1 IVL's can be very large in the case of photoionization pumping, leading to a huge gain (a few tens per cm or larger), as discussed below.

In this paper, the gain characteristics of the $L_{23}M_1$ innershell transition of Ca in the case of x-ray photopumping are presented. The transition wavelength is at 4.1 nm, which is inside the water window and therefore may be particularly useful for holographic imaging or high-resolution microscopy of biological samples *in vivo* [23]. Among the elements suggested in Ref. [10], Ca has been chosen in this study because Ca has (1) a higher gain cross section, (2) longer lifetime of the upper level, and (3) smaller absorption coefficient at the lasing wavelength. These attributes of Ca lead to a larger net effective gain. Figure 1 shows the energy levels considered in the simulations: one neutral level, six single IVL's, and 21 double IVL's (when energy differences for levels are small, they are treated as one level). Figure 1 does not show all the levels included in the simulations. Populations are calculated only for the single IVL's. The double IVL's are considered for two reasons: to include the
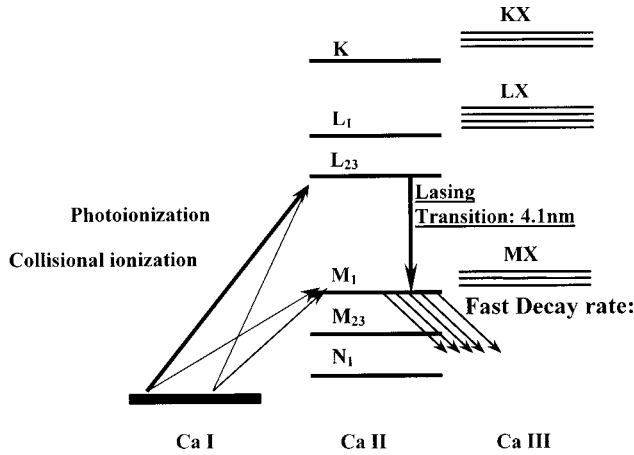
FIG. 1. Schematic energy level diagram of inner-shell-vacancy levels in Ca used in the simulation.

decay channels from the single IVL's such as photoionization, electron collisional ionization, and Auger and Coster–Kronig decay; and to calculate the energy distribution of generated electrons. Radiative decay channels are included among single IVL's. All the Auger and Coster–Kronig decay, photoionization, and electron-collisional ionization channels from single IVL's to possible double IVL's are considered. The electron-collisional ionization rate is evaluated using an electron energy distribution calculated during the simulation. In the gain calculation, the natural linewidth is used, because both Stark broadening and Doppler broadening are smaller under the circumstances considered in this paper.

Figure 2 shows simulation results for pumping radiation at 360 eV with different power densities and pulse durations. The initial neutral density of Ca used is 1.2×10^{21} cm^{-3}. The time $t = 0$ is the time when a pumping radiation reaches its maximum. The time evolution of the populations of various single IVL's for a Gaussian pulse of 10 fs full width at half-maximum (FWHM) with a radiation flux of 1.4×10^{19} photons/cm^2 is shown in Fig. 2(a). The pumping photon's energy of 360 eV is slightly larger than the L_{23} absorption edge in Ca. The photoionization cross section for $2p$ electrons is larger than that for electrons in other orbitals (in other words, the pumping rate to the L_{23} IVL is the largest). On the other hand, the decay from the M_1 IVL caused by Coster–Kronig process is so fast that the population of the M_1 IVL is negligible. These lead to a population inversion between the L_{23} and M_1 IVL's from the beginning of the pumping radiation.

In Fig. 2(b), the variation of gain on the $L_{23}M_1$ transition is plotted for the same condition as in Fig. 2(a). G_{inv} is the gain due to population inversion, and G_{eff} is the effective gain, i.e., the difference between G_{inv} and the absorption of the lasing line by neutrals and ions: $G_{eff} = G_{inv} - \alpha_{abs}$. A large G_{inv} is obtained almost from the beginning of the pumping radiation pulse even before the pumping radiation reaches its maximum. However, at this early stage the absorption is still large, preventing amplification. Later when the upper level is sufficiently populated, G_{eff} becomes positive. The maximum of the effective gain occurs earlier than
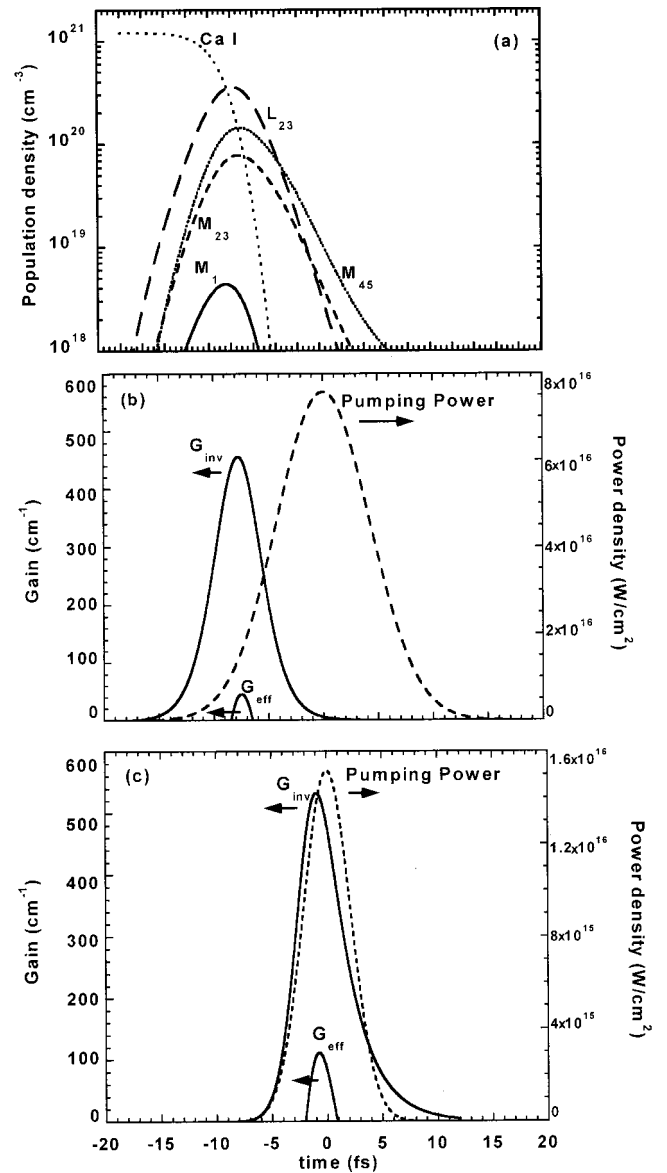

FIG. 2. (a) Temporal change of the population of Ca I and inner-shell-vacancy levels in Ca II. The initial neutral density of Ca used is 1.2×10^{21} cm^{-3}. The time variation of the populations of various single IVL's for a Gaussian pulse of 10 fs FWHM with a radiation flux at 360 eV of 1.4×10^{19} photons/cm^2. (b) Temporal change of G_{inv} and G_{eff} for the same condition as in (a). (c) Temporal change of G_{inv} and G_{eff} for a shorter (5 fs) and smaller pumping power than in (b).

that of the pumping radiation. Pumping power density around $t = -12$ fs is already large enough to significantly populate the L_{23} IVL level (creating a large population inversion). As the pumping continues, the neutrals are depleted rapidly [Fig. 2(a)] so that by the time of $t = -7$ fs few neutrals remain. The population of the L_{23} IVL then begins to decrease because the pumping to the level ceases. When the pumping radiation reaches its maximum, the gain becomes negligible. In this particular case, at least the second half of the pumping flux does not make any contribution to the population inversion and is wasted. For more efficient use of photons, there are two ways to make the gain maximum

occur at the same time when the pumping radiation reaches its maximum; to reduce either the power or duration of the pumping radiation. The reduction of pumping power leads to the smaller or no gain, which is not useful for experimental realization.

Figure 2(c) shows a simulation of shorter pulse duration (5 fs FWHM) pumping with even a smaller pumping flux. A higher gain relative to the previous case is achieved around the maximum of the pumping radiation. The magnitude of G_{eff} is much smaller than that of G_{inv} but still large compared to typical x-ray laser schemes. The positive effective gain exists only during a small portion of the pumping (~ 3 fs [Figs. 2(b) and 2(c)]). Singly inner-shell ionized or doubly inner-shell ionized ions still absorb the lasing transition because they still have $3p$ electrons. The gain cross section of the $L_{23}M_1$ lasing transition is only about three times larger than the absorption cross section at this wavelength. No positive effective gain is achieved until the L_{23} IVL is sufficiently populated to overcome the absorption. These facts lead to a shorter duration for G_{eff} than for G_{inv}.

The behavior of the maximum values of G_{inv} and G_{eff} with respect to the initial Ca density for a given radiation flux of 1×10^{18} photons/cm^2 and a duration of 2 fs FWHM is shown in Fig. 3(a). The maximum of G_{inv} monotonically increases less than linearly with the initial density. This is due to the depletion of neutrals by collisional ionization process of Auger and photoelectrons, which is against the formation of population inversion, as discussed below. Figure 3(b) depicts photoionization rates to the L_{23} IVL, collisional ionization rates to the M_1, M_{23}, and N_1 IVL's at the time of the gain maximum for the same pumping flux as in Fig. 3(a). The photoionization rate at the time of the gain maximum (P_{L23}) decreases, because the gain maximum occurs earlier for a given pump power as the initial density increases. On the contrary, as the density increases, the collisional ionization rates at the time of gain maximum (C_{M1}, C_{M23}, and C_{N1}) increases because more Auger and photoelectrons are liberated. Hence as the density increases, collisional ionization processes become good channels for the depletion of neutrals, hindering the increase of G_{inv}. Virtually all materials, either neutrals or ions, absorb the lasing transition so that absorption increases linearly with density. These behaviors result in the fact that G_{eff} has a maximum and there exists a critical density n_{cr}, for a given pumping power of radiation, beyond which no positive effective gain is achieved. This critical density occurs when the photoionization rate becomes equal to the collisional ionization rate at the time of gain maximum when the pumping duration is equal to or less than the lifetime of the upper level. In this particular case for the conditions of Fig. 3, $n_{\text{cr}} = 1.3 \times 10^{22}$ cm^{-3}. This critical density is a function of pumping flux and duration. It becomes larger with a larger pumping flux and a shorter pumping duration. For example, for a duration of 2 fs FWHM and a pumping flux of 10^{19} photons/cm^2, n_{cr} occurs at 2.1×10^{22} cm^{-3}; for a duration of 5 fs FWHM and a pumping flux of 10^{18} photons/cm^2, n_{cr} occurs at 2.1×10^{21} cm^{-3}. A higher gain is achieved for higher critical density.

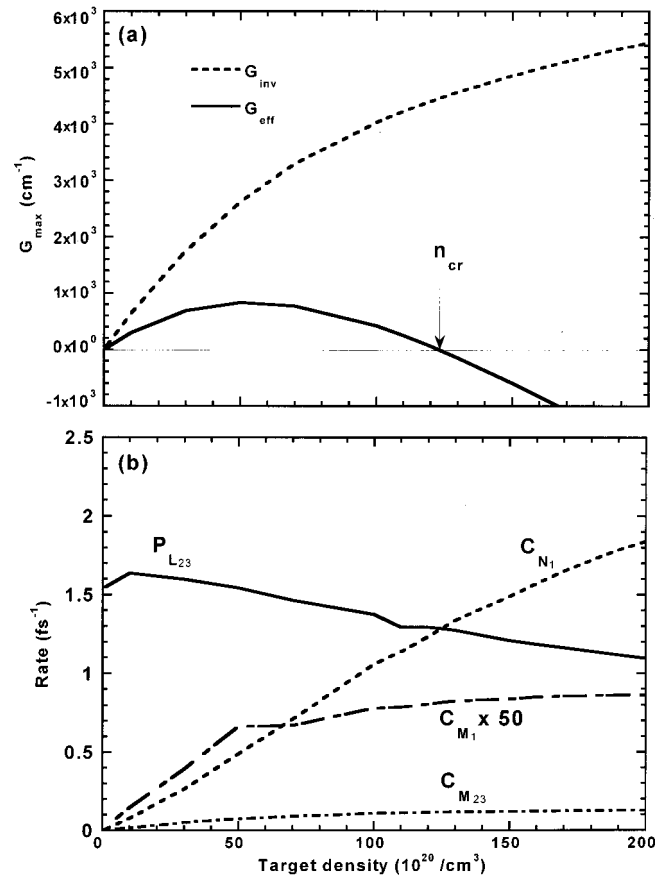Since the lifetime of the lower level (0.8 fs for M_1 IVL in

FIG. 3. (a) Behavior of the maxima of G_{inv} and G_{eff} with respect to the initial Ca density for a given radiation flux of 1×10^{18} photons/cm^2 and a duration of 2 fs FWHM. (b) Behavior of photoionization rates for the L_{23} IVL (P_{L23}), collisional ionization rates for the M_1, and M_{23}, IVLs (C_{M1}, C_{M23}) at the time of the gain maximum for the same pumping flux as in (a).

Ca) is much shorter than that of the upper level (3.5 fs for L_{23} level in Ca), population inversion can be created with the radiation source of relatively long pulse durations, even as long as 1-ps pulse (Fig. 4). This is an important advantage of the $L_{23}M_1$ transition compared to a KL transition. In the case of KL transitions, the lifetime of the lower level (L IVL) is much longer than that of the upper level (K IVL). According to Ref. [11], no inversion between the K and L IVL's in carbon can be created for a radiation pulse longer than 80 fs at any power.

Up to now, the gain characteristics of the $L_{23}M_1$ transition when pumped by a monochromatic source has been discussed. This is helpful to understand the behavior of the transition but in reality there is no monochromatic source. Taking black-body radiation as a polychromatic source, a series of simulations have been done. One of typical examples is shown in Fig. 5 where the black body temperature is 9 keV. This temperature is taken to have the similar photon flux at 360 eV (energy bandwidth: 10 eV and solid angle: 2π) to that in the case of a high gain with a monochromatic source. Figure 5(a) shows the behavior of the inversion gain and effective gain. Due to the rapid decay of the $M1$ vacancy level, the population inversion is established but not enough
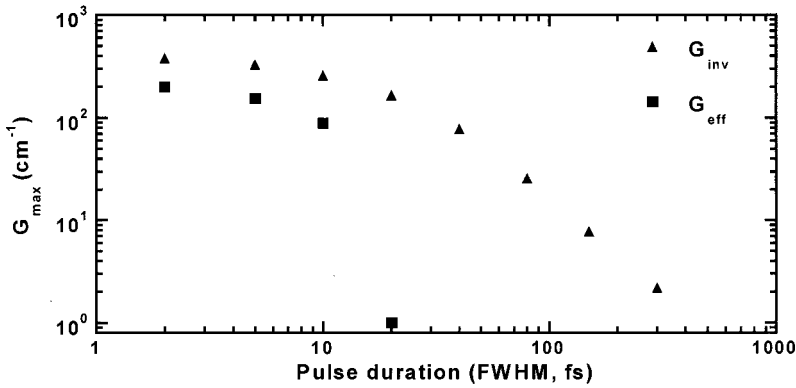
FIG. 4. Change of gain with respect to the pulse duration of pumping x-ray flux of 10^{20} photons/cm^2. The initial Ca density is 5 $\times 10^{20}$ cm^{-3}.

to overcome the absorption: there is no positive effective gain. This can be understood by looking at the spectrum of the black-body radiation. The spectrum of the black-body radiation at $T_b = 9$ keV is shown in Fig. 5(b). As can be seen, there are too many high-energy photons, which produce many extra electrons. These electrons enhance the depletion of neutrals, preventing the large degree of population inversion: inversion is established due to the fast decay of $M1$

inner-shell vacancy state but not enough to overcome the absorption. When the black-body temperature is lowered to reduce the number of high-energy photons, the photon flux at 360 eV is not so sufficient that no positive effective gain is achieved, either.

We have considered another polychromatic radiation source: the laser Larmor radiation [24], which is the radiation by relativistic electrons under ultrahigh field. This radiation is intense, directed due to the relativistic motion of electrons. Most importantly, the duration of this radiation is on the order of an optical driving laser pulse. Its bandwidth is narrow compared to that of black-body radiation as shown in Fig. 6, where the black-body temperature and the laser parameter are adjusted that each source has similar radiation flux at 360 eV. This radiation source can generate the suffi-
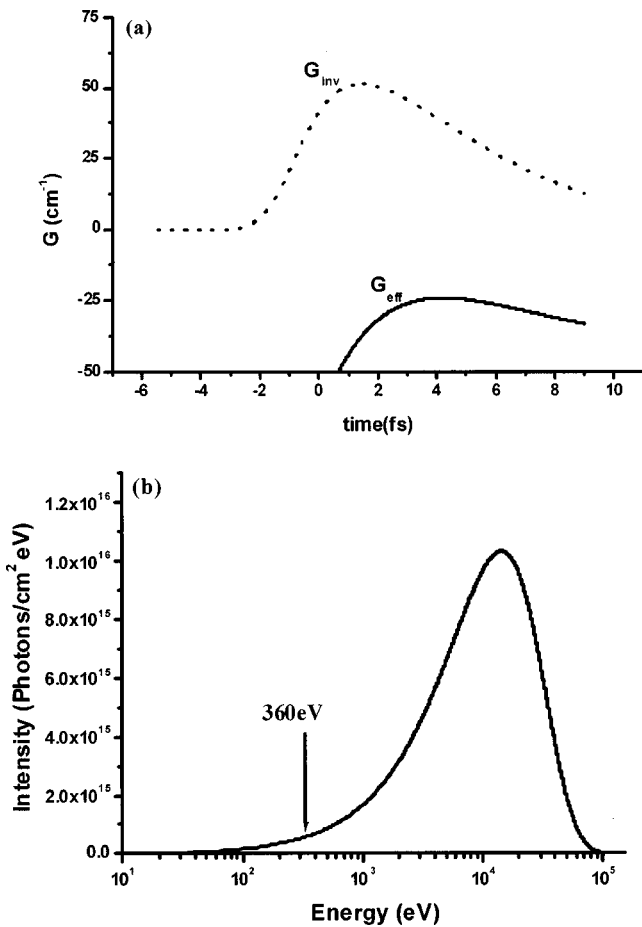

FIG. 5. (a) Temporal change of G_{inv} and G_{eff} for the black-body radiation with a temperature of 9 keV and a duration of 5 fs FWHM. (b) The energy distribution of the black-body radiation used in (a). The photon energy of 360 eV indicated by the arrow is slightly above the L_{23} absorption edge of Ca.
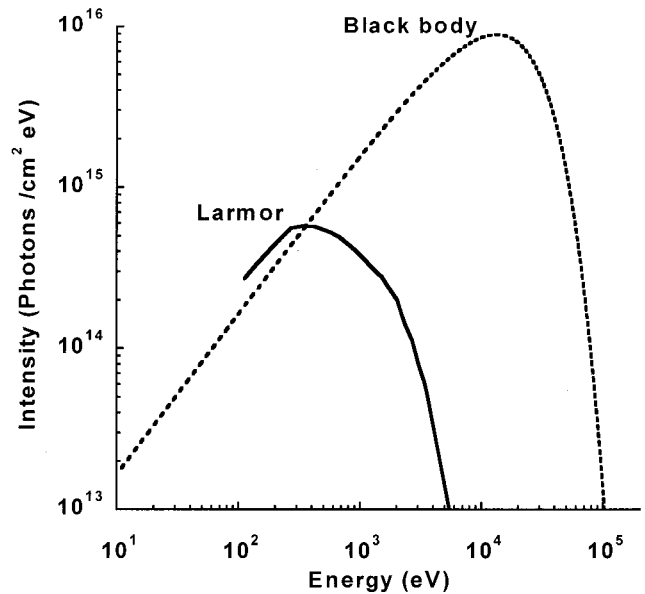

FIG. 6. Comparison of the energy distributions of the black-body radiation at $T_b \cong 9$ keV and laser Larmor radiation with a laser strength parameter of $a_0 = 10$. The laser strength parameter is defined by the ratio of the maximum quiver velocity to the speed of light: $a_0 \equiv eE_0/m_e c \, \omega_L$, where e, m_e, c, E_0, and ω_L represent the electron charge, rest mass, speed of light, the maximum strength of the electric field, and laser frequency. A laser strength parameter of $a_0 = 10$ is equivalent to a laser intensity in the range of 1 $\times 10^{18}$ W/cm^2 for visible and near infrared wavelengths.
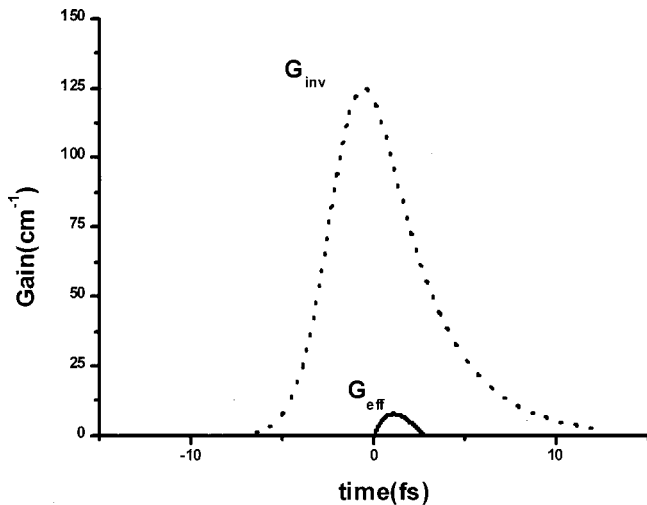
FIG. 7. Temporal change of G_{inv} and G_{eff} for pumping with the laser Larmor radiation characterized by a laser strength parameter of $a_0=10$, a duration of 5 fs FWHM and energy bandwidth of 360 to 500 eV. The initial Ca density is 5×10^{20} cm^3.

cient degree of population inversion to produce the effective gain as shown in Fig. 7. This laser Larmor radiation has also been considered as a pumping radiation source by others [25].

Simulations reveal that for a photon flux of 2.4 $\times10^{18}$ photons/cm^2 at the energy of 360 eV with a risetime of 12 fs, $G_{eff}=\sim65$ cm^{-1} is expected for an initial Ca density of 8×10^{20} cm^{-3}. For GL=5, the estimated output intensity of the $L_{23}M_1$ transition at 4.1 nm in Ca is about 2 $\times10^{28}$ photons/cm^2 s. The estimated x-ray pump energy at 360 eV required for the above system assuming a gain region of 10 μm by 0.8 mm is about 11 mJ. Using a conversion efficiency of 0.1% from visible photons to x-ray photons under interest [11], the required energy of an optical drive laser is about 11 J. In another case of a rise time of 5 fs with a photon flux at 360 eV of 8.5×10^{17} photons/cm^2, $G_{eff}=\sim110$ cm^{-1} is expected for an initial Ca density of 1.2 $\times10^{21}$ cm^{-3}. For GL=10, the output intensity is estimated to be about 2×10^{30} photons/cm^2 s. The peak spectral brightness of this output is about 5×10^{25} photons/s/ (mm^2 mrad^2 0.1% bandwidth), which is 4 or 5 orders of magnitude brighter than a typical undulator radiation in the similar spectral region, and 2 or 3 orders of magnitude brighter than the saturated output of a collisionally pumped Ne-like Se laser at 20.6 and 20.9 nm [26]. For the above system, the estimated x-ray pump energy at 360 eV required is about 5 mJ for a gain region of 10 μm by 1 mm. Assuming

a conversion efficiency of 0.1% from visible photons to x-ray photons, the required energy of an optical drive laser is about 5 J. The above estimations are based on a monochromatic pumping radiation source. Hence they set the lower limit to the required energy of a driving pump laser for an assumed conversion efficiency. Recent experiments show that the conversion efficiency of visible photons to x-ray photons is in the range of a few to about 20% from flat solid [27,28], structured solid [29], and cluster [30] targets. All of these experiments have been done with laser pulses of longer than 100 fs and have shown instrument-limited time duration on the x-ray burst. We have used the conversion efficiency of 0.1%, which is the result of LASNEX simulation in the similar spectral region [11].

No experimental work has been reported yet on the conversion efficiency to x rays when a 10 fs TW laser interacts with matter. Ultraintense laser-matter interaction is just an emerging field. Radiation characteristics of matter under this circumstance has to be further investigated. Characterization of the flux and rise time of x rays in 10 fs TW high-intensity laser/matter interactions is presently underway, among others, at University of California, San Diego (UCSD), Lawrence Livermore National Lab. and IQE-FSU, Jena, Germany.

In conclusion, we have investigated the gain and population dynamics for the first time of the Ca $L_{23}M_1$ transition in the case of x-ray photoionization pumping. We have shown that very high gain can be achieved and have demonstrated that there exists an optimal density of target atom for the highest gain for a given pumping power. The expected laser pulse duration is <10 fs. The saturation fluence of the Ca $L_{23}M_1$ transition is high so that if saturation be achieved, i.e., GL>~15, the peak spectral brightness of the Ca $L_{23}M_1$ laser would be several orders of magnitude higher than present undulator sources. Water window sources of this brightness and ultrafast time duration should be extremely useful for *in vivo* high-resolution microscopic and holographic studies of biological phenomena. It has been shown that conventional pump sources such as black-body radiation cannot achieve the effective gain. The radiation characteristics of plasmas created by high power femtosecond lasers needs to be further studied. The laser Larmor radiation, which looks promising, needs to be also experimentally demonstrated.

[1] B. C. Walker, C. Tóth, D. N. Fittinghoff, T. Guo, D. Kim, C. Rose-Petruck, J. Squier, K. Yamakawa, K. R. Wilson, and C. P. J. Barty, Opt. Express **5**, 196 (1999).

[2] K. Yamakawa, M. Aoyama, S. Matsuoka, T. Kase, Y. Akahane, and H. Takuma, Opt. Lett. **23**, 1468 (1998).

[3] C. P. J. Barty, T. Guo, C. Le Blanc, F. Raksi, C. Rose-Petruck,

J. Squire, K. R. Wilson, V. V. Yakovlev, and K. Yamakawa, Opt. Lett. **21**, 668 (1996).

[4] J. P. Chambaret, C. Le Blanc, G. Cheriaux, P. Curley, G. Darpentigny, P. Rousseau, G. Hamoniaux, A. Antonetti, and F. Salin, Opt. Lett. **21**, 921 (1996).

[5] M. Schnürer, Ch. Spielmann, P. Wobrauschek, C. Streli, N. H.

Burnett, C. Kan, K. Ferencz, R. Koppitsch, Z. Cheng, T. Brabec, and F. Krausz, Phys. Rev. Lett. **80**, 3236 (1998).

[6] A. Rundquist, C. G. Durfee III, Z. Chang, C. Herne, S. Backus, M. M. Murnane, and H. C. Kapteyn, Science **280**, 1412 (1998).

[7] Y. Tamaki, J. Itatani, Y. Nagata, M. Obara, and K. Midorikawa, Phys. Rev. Lett. **82**, 1422 (1999).

[8] H. J. Shin, D. G. Lee, Y. H. Cha, K. H. Hong, and C. H. Nam, Phys. Rev. Lett. **83**, 2544 (1999).

[9] J. J. Macklin, J. D. Kmetec, and G. L. Gordon III, Phys. Rev. Lett. **70**, 766 (1993).

[10] D. Kim, C. Tóth, and C. P. J. Barty, Phys. Rev. A **59**, R4129 (1999).

[11] S. J. Moon and D. C. Eder, Phys. Rev. A **57**, 1391 (1998).

[12] K. Moribayashi, A. Sasaki, and T. Tajima, Phys. Rev. A **58**, 2007 (1998).

[13] Y. Li, H. Schillinger, C. Ziener, and R. Sauerbrey, Opt. Commun. **144**, 118 (1997).

[14] D. L. Matthews, in *X-ray Lasers 1996*, IOP Conf. Series 151 (IOP, Bristol, 1996), p. 32.

[15] G. L. Strobel, R. A. London, and D. C. Eder, Appl. Phys. B: Lasers Opt. **60**, 513 (1995).

[16] H. Kapteyn, Appl. Opt. **31**, 4931 (1992).

[17] C. Rose-Petruck, R. Jimenez, T. Guo, A. Cavalleri, C. W. Siders, F. Ráksi, J. A. Squier, B. C. Walker, K. R. Wilson, and C. P. J. Barty, Nature (London) **398**, 310 (1997).

[18] A. Duguay and P. M. Rentzepis, Appl. Phys. Lett. **10**, 350 (1967).

[19] Y. L. Stankevich, Sov. Phys. Dokl. **15**, 356 (1970)].

[20] F. T. Arecchi, G. P. B. Banfi, and A. M. Malvezzi, Opt. Commun. **10**, 214 (1974).

[21] R. C. Elton, Appl. Opt. **14**, 2243 (1975).

[22] T. S. Axelrod, Phys. Rev. A **13**, 376 (1976).

[23] R. London, M. D. Rosen, and J. E. Trebes, Appl. Opt. **28**, 3397 (1989), and references therein.

[24] Y. Ueshima, Y. Kishimoto, A. Sasaki, and T. Tajima, Laser Part. Beams **17**, 45 (1999).

[25] K. Moribayashi, A. Sasaki, and T. Tajima, Phys. Rev. A **58**, 2007 (1998); **59**, 2732 (1999).

[26] T. N. Lee, S. H. Kim, and H. J. Shin, J. Korean Phys. Soc. **33**, 228 (1998).

[27] J. A. Cobble, G. T. Schappert, L. A. Jones, A. J. Taylor, G. A. Kyrala, and R. D. Fulton, J. Appl. Phys. **69**, 3369 (1991).

[28] J. A. Cobble, G. A. Kyrala, A. A. Hauer, A. J. Taylor, C. C. Gomez, N. D. Delamater, and G. T. Schappert, Phys. Rev. A **39**, 454 (1989).

[29] M. M. Murnane, H. C. Kapteyn, S. P. Gordon, J. Bokor, E. N. Glytsis, and R. W. Falcone, Appl. Phys. Lett. **62**, 1068 (1993).

[30] T. Ditmire, T. Donnelly, R. W. Falcone, and M. D. Perry, Phys. Rev. Lett. **75**, 3122 (1995).